General Disclaimer

One or more of the Following Statements may affect this Document

- This document has been reproduced from the best copy furnished by the organizational source. It is being released in the interest of making available as much information as possible.

- This document may contain data, which exceeds the sheet parameters. It was furnished in this condition by the organizational source and is the best copy available.

- This document may contain tone-on-tone or color graphs, charts and/or pictures, which have been reproduced in black and white.

- This document is paginated as submitted by the original source.

- Portions of this document are not fully legible due to the historical nature of some of the material. However, it is the best reproduction available from the original submission.

Produced by the NASA Center for Aerospace Information (CASI)

NASA Technical Memorandum 83319

(NASA-TM-83319) SPECIMEN SIZE AND GEOMETRY EFFECTS ON FRACTURE TOUGHNESS OF A1203 MEASURED WITH SHORT ROD AND SHORT BAR CHEVRON-NOTCH SPECIMENS (NASA) 14 p HC A02/MF A01 CSCL 07C G3/27 N83-19902 Unclas 03126

Specimen Size and Geometry Effects on Fracture Toughness of Al_2O_3 Measured With Short Rod and Short Bar Chevron-Notch Specimens

John L. Shannon, Jr.
Lewis Research Center
Cleveland, Ohio

and

Dietrich G. Munz
University of Karlsruhe
D-75 Karlsruhe 1, FR (West) Germany

Prepared for the
Symposium on Chevron-Notched Specimens:
Testing and Stress Analysis
sponsored by the American Society for Testing and Materials
Louisville, Kentucky, April 21, 1983

NASA

SPECIMEN SIZE AND GEOMETRY EFFECTS ON FRACTURE TOUGHNESS OF Al_2O_3 MEASURED WITH SHORT ROD AND SHORT BAR CHEVRON-NOTCH SPECIMENS

John L. Shannon, Jr.

National Aeronautics and Space Administration
Lewis Research Center
Cleveland, Ohio 44135

Dietrich G. Munz

University of Karlsruhe
D-75 Karlsruhe 1
FR (West) Germany

E-1560

SUMMARY

Plane strain fracture toughness measurements were made on Al_2O_3 using short rod and short bar chevron-notch specimens previously calibrated by the authors for their dimensionless stress intensity factor coefficients. The measured toughness varied systematically with variations in specimen size, proportions, and chevron notch angle apparently due to their influence on the amount of crack extension to maximum load (the measurement point). The toughness variations are explained in terms of a suspected rising R-curve for the material tested, along with a discussion of an unavoidable imprecision in the calculation of K_{Ic} for materials with rising R-curves when tested with chevron-notch specimens.

NOMENCLATURE

a		crack length
Δa		crack extension
a_m		crack length at minimum of Y*
a_{max}		crack length at P_{max}
a_o		initial crack length (distance from line of load application to tip of chevron)
a_1		length of chevron notch at specimen surface (distance from line of load application to point of chevron emergence at specimen surface)
α	=	a/W
$\Delta\alpha$	=	$\Delta a/W$
α_m	=	a_m/W
α_{max}	=	a_{max}/W

a_o = a_o/W

a_1 = a_1/W

B thickness of short bar specimen or diameter of short rod specimen

b crack front length

b_m crack front length at minimum of Y*

K stress intensity factor

K_{Ic} plane strain fracture toughness

K_{IR} crack extension resistance

K_{IR_m} crack extension resistance at minimum of Y*

$K_{IR_{max}}$ crack extension resistance at P_{max}

P load

P_m load at minimum of Y*

P_{max} maximum load

W specimen width

Y* dimensionless stress intensity factor coefficient for a trapezoidal crack, = $KB\sqrt{W}/P$

Y^*_m minimum of Y* as function of α

Y^*_{max} Y* at P_{max}

INTRODUCTION

The performance of short bar and four-point-bend chevron-notch specimens in measuring the fracture toughness of aluminum oxide, using experimentally and analytically determined stress intensity factor calibrations, has been previously reported upon by the authors [1] to [3]. The measured fracture toughness varied systematically with variations in specimen size, proportions, and chevron notch angle apparently due to their influence on the amount of crack extension to maximum load (the measurement point). Similar effects would be expected for the short rod chevron-notch specimen, first used by Barker [4].

Experimentally determined stress intensity factor calibrations of the short rod specimen have recently been made by the authors to enable calculation of fracture toughness from maximum test load [5] and [6]. These calibrations were used for the short rod specimens in this study. Fracture toughness tests were made on the same Al_2O_3 stock that was used in the investigations reported upon in references [1] to [3]. The short bar specimen results of references [1] and [3] are combined with the short rod specimen results newly reported here for the sake of generalizing conclusions on size and geometry effects for the chevron-notch type of fracture toughness specimen.

EXPERIMENTAL MATERIAL, SPECIMENS, AND PROCEDURE

The experimental material used in this investigation of the short rod chevron-notch specimen was from the same production of 3M Company Alsimag-614 sintered aluminum oxide (Al_2O_3) as that used in the studies of references [1] to [3]. Short rod specimens were machined to the dimensions shown in figure 1 from cylindrical blanks 12.7 mm and 25.4 mm in diameter. Width-to-diameter (W/B) ratios of both 1.5 and 2.0 were examined. The chevron notch length at the specimen surface (a_1) was always made equal to the specimen width (W), (i.e., $a_1 = 1$). The chevron angle was varied by varying the length to the chevron tip (a_0). The notches were introduced by diamond wheel slotting with kerfs (slot width, N) of either 0.4 mm or 1.0 mm depending on the specimen diameter.

Results for the short bar specimens reported in references [1] and [3] are repeated here. Those specimens were machined to the dimensions shown in figure 2 from rectangular blanks of 12.7 mm and 25.4 mm square cross section. Like the short rod specimens, proportions (width-to-height, W/2H ratios) of both 1.5 and 2.0 were produced. Chevron angles were varied by varying either a_0 or a_1. The notches were introduced either by diamond coated wire sawing or diamond wheel slotting. Slot widths in the 12.7 mm thick specimens were 0.25 mm. Those in the 25.4 mm thick specimens were either 0.25 mm or 0.70 mm. As pointed out in references [1] and [3], no effect of slot width was observed for these 25.4 mm thick specimens.

The test setup, shown schematically in figure 3, was the same as that used in references [1] and [3]. Care was exercised in aligning the loading rods according to a procedure previously used by the authors for compliance calibrations of the short bar [7] and short rod [5] specimens. A double-cantilever displacement gage (ASTM Standard Method of Test for Plane-Strain Fracture Toughness of Metallic Materials E-399-81) was inserted into knife edges integral with the loading rods, as shown in figure 3. The displacement gage force was tared from the load measurement, and the specimen was installed by pressing it firmly against the loading rods to seat the loading knife edges in the corners of the recessed notch mouth of the specimen.

Specimen load was applied at a constant test machine crosshead speed of 0.05 mm/min. A typical load versus displacement record is shown in figure 4. The slope of the record trace is initially depressed because of local surface damage to the specimen at the loading knife edge line of contact, but increases continuously to become linear, and thereafter decreases with stable crack extension. After passing through its maximum, the trace suddenly drops because of rapid specimen fracture.

For material with a flat crack growth resistance curve (R-curve)[1], the chevron-notch specimen fracture toughness is proportional to the maximum load as expressed in the following:

$$K_{Ic} = \frac{P_{max}}{B\sqrt{W}} Y_m^* \qquad \text{(see footnote 2)} \qquad (1)$$

where Y_m^* is the minimum value of the dimensionless stress intensity factor coefficient as a function of relative crack length for the particular specimen used (i.e., for the particular specimen proportions W/B for the short rod specimen and W/2H for the short bar specimen, and chevron notch parameters a_0 and a_1). From the experimental compliance calibrations of references [5] and [6], the

following polynomial expression for Y_m^* for short rod chevron-notch specimens with $a_1 = 1$ was developed for use in the present investigation:

$$Y_m^* = 19.98 - 9.54(W/B) + 6.80(W/B)^2 + \left[-118.7 + 125.1(W/B) - 22.08(W/B)^2\right] a_o + \left[379.4 - 363.6(W/B) + 84.4\,(W/B)^2\right] a_o^2 \quad (2)$$

RESULTS AND DISCUSSION

As expected, the short rod specimen results of this investigation (figure 5) closely resemble the short bar specimen results previously obtained by the authors [1]. There is little if any perceptible influence of a_o on K_{Ic} within the range investigated, but a measureable effect of specimen size and proportions, B and W/B. As explained previously for the short bar specimen [1], these effects can be ascribed to a rising R-curve for the aluminum oxide material tested. Specimen size, proportion, and chevron notch angle all affect the amount of crack extension to maximum load (the measurement point), and therefore K_{Ic} as dictated by the shape of the R-curve.

As the crack proceeds down the chevron shaped ligament, the test load passes through a smooth maximum. For materials with flat R-curves, this maximum occurs at the same relative crack length where the corresponding dimensionless stress intensity factor calibration curve (Y* versus a) exhibits a minimum, namely a_m. This value of Y* is designated Y_m^* and is used in equation (1) to compute K_{Ic} directly from maximum load.

For any flat R-curve material, the crack extension to maximum load is $(a_m - a_o)$. a_m is not measured on the specimen, but is computed as W times a_m, where a_m is read from the Y* versus a curve for that specimen at Y_m^*.

For materials with rising R-curves, maximum load and Y_m^* do not occur coincidently at a_m. The load peaks, instead, at a relative crack length greater than a_m. This results in some error in the calculation of K_{Ic} at maximum load because we do not know the corresponding value of crack length. Nevertheless, a plot of K_{Ic} versus $(a_m - a_o)$ should be a reasonable approximation of the basic trend of the fracture resistance versus crack extension to maximum load curve and serve as an indication of whether the material has a flat R-curve or not.

Figure 6 is the K_{Ic} versus $(a_m - a_o)$ curve for the short rod specimen, and figure 7 is the corresponding curve for the short bar specimen reported upon previously [1]. These curves are not R-curves, but rather the loci of points lying on a family of R-curves, with each R-curve being specific to the particular chevron-notch specimen involved. In effect, the chevron-notch is a variably side-grooved specimen. As the crack proceeds down the chevron, the constraint provided by the notch varies, and how it varies will depend on the particular geometry of the chevron. Thus we can imagine that the data in figure 7, for example, are specific

points on a family of R-curves as shown schematically in figure 8.

For each of the two curves in figure 7, one chevron notch parameter (either α_0 or α_1) was fixed while the other was varied. K_{Ic} at a given value of crack extension to maximum load is different in the region of lesser extensions due to the different constraint afforded by the two manners of adjusting the chevron angle. The data can be normalized to account for the variable side grooving effect by multiplying the crack extension by $(B - b_m)/B$ as shown in figure 9, where all the data falls on a common curve.

The difficulty in calculating K_{Ic} for materials with rising R-curves can be understood as follows. From an energy consideration, crack extension in the chevron-notch specimen occurs so as to satisfy the following relation [7]:

$$K_{IR} = \frac{P}{B\sqrt{W}} \; Y^* \tag{3}$$

For a given material the K_{IR} versus Δa curve is fixed, and for a given specimen geometry the Y^* versus Δa curve is fixed. The P versus Δa curve then follows directly from equation (3).

The consequence of a rising R-curve is not just to raise the load for continued crack extension compared to that dictated by a flat R-curve, but also to shift the load maximum with respect to the Y^* curve minimum as shown schematically in figure 10. As seen for a hypothetical rising R-curve, and a typically shaped Y^* curve, P_{max} occurs at a relative crack length α_{max} greater than α_m corresponding to the Y^* curve minimum. Referring still to figure 10, K_{IR_m} and $K_{IR_{max}}$ are computed using the following combinations of load and stress intensity factor coefficients:

$$K_{IR_m} = \frac{P_m \cdot Y^*_m}{B\sqrt{W}} \quad \text{and} \quad K_{IR_{max}} = \frac{P_{max} \cdot Y^*_{max}}{B\sqrt{W}}$$

Calculation of K_{Ic} is conventionally done on the assumption of a flat R-curve using the following combination of P and Y^*:

$$K_{Ic} = \frac{P_{max} \cdot Y^*_m}{B\sqrt{W}}$$

K_{Ic} calculated in this way yields a value which lies on the R-curve between K_{IR_m} and $K_{IR_{max}}$, this uncertainty being greater the steeper the R-curve. Since it is reasonable to assume that K_{IR} depends on the absolute amount of crack extension Δa and not the relative amount $\Delta\alpha$, K_{Ic} from proportionate chevron-notch specimens can be expected to increase with increasing specimen size.

FOOTNOTES

[1]Plot of crack extension resistance K_{IR} versus crack extension Δa.

[2]The authors recognize that the designation K_{Ic} is customarily reserved for that value of plane strain fracture toughness determined in strict accordance with ASTM Standard Test Method for Plane-Strain Fracture Toughness of Metallic Materials (E-399). For materials with flat crack growth resistance curves, we believe the chevron-notch specimen would yield a plane strain fracture toughness value fully equivalent to K_{Ic} of the E-399 test and without the encumbrances of posttest crack length measurement and secant-line construction on the test record. For materials with nonflat crack growth resistance curves, as suspicioned for the Al_2O_3 material tested here, the measured K_{Ic} will be different from the E-399 value, but is nevertheless designated K_{Ic} in this paper for convenience.

REFERENCES

[1] Munz, D., Bubsey, R. T., and Shannon, J. L., Jr., Journal of Testing and Evaluation, Vol. 8, No. 3, May 1980, pp. 103-107.

[2] Munz, D., Bubsey, R. T., and Shannon, J. L., Jr., Journal of the American Ceramics Society, Vol. 63, No. 5-6, May-June 1980, pp. 300-305.

[3] Shannon, J. L., Jr., Bubsey, R. T., Munz, D., and Pierce, W. S., In Advances in Fracture Research, D. Francois, Ed., Pergamon Press, New York, 1982, pp. 1127-1141.

[4] Barker, L. M., Engineering Fracture Mechanics, Vol. 9, No. 2, 1977, pp. 361-369.

[5] Bubsey, R. T., Munz, D., Pierce, W. S., and Shannon, J. L., Jr., International Journal of Fracture, Vol. 18, No. 2, Feb. 1982, pp. 125-133.

[6] Shannon, J. L., Jr., Bubsey, R. T., Pierce, W. S., and Munz, D., International Journal of Fracture, Vol. 19, No. 3, July 1982, pp. R55-R58.

[7] Munz, D., Bubsey, R. T., and Srawley, J. E., International Journal of Fracture, Vol. 16, No. 4, August 1980, pp. 359-374.

ORIGINAL PAGE IS
OF POOR QUALITY

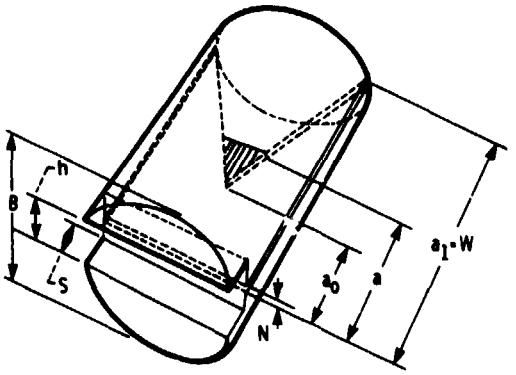

DIMENSIONS OF SPECIMENS TESTED IN THIS INVESTIGATION							
B	W	W/B	h	S	N	a_0	a_1
25.4	50.8	2.0	6.4	3.8	1.0	12.5-22.5 (SIX SPECIMENS)	50.8
25.4	38.1	1.5	6.4	3.8	1.0	7.5-16.0 (TEN SPECIMENS)	38.1
12.7	25.4	2.0	6.4	3.8	0.4	4.5-10.0 (EIGHT SPECIMENS)	25.4
12.7	19.1	1.5	6.4	3.8	0.4	3.4-7.9 (NINE SPECIMENS)	19.1

ALL DIMENSIONS IN mm.

Figure 1. - Chevron-notch short rod fracture toughness test specimen.

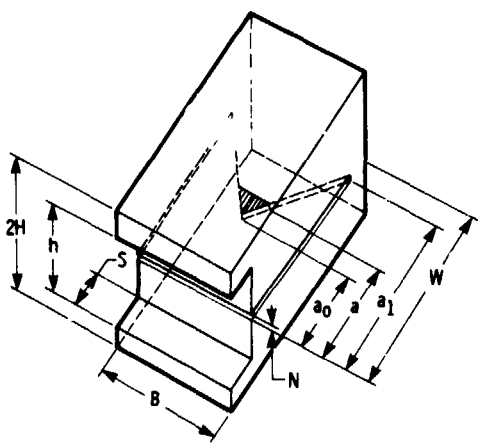

DIMENSIONS OF SPECIMENS TESTED IN INVESTIGATIONS OF REFERENCES (1) AND (3)								
B	W	2H	W/2H	h	S	N	a_0	a_1
25.4	50.8	25.4	2.0	12.7	3.8	0.25 or 0.70	10.6-22.2 (NINE SPECIMENS)	50.8
25.4	38.1	25.4	1.5	12.7	3.8	0.25 or 0.70	8.6-17.6 (NINE SPECIMENS)	38.1
12.7	25.4	12.7	2.0	6.3	3.8	0.25	4.8-11.5 (TEN SPECIMENS)	25.4
12.7	25.4	12.7	2.0	6.3	3.8	0.25	5.1 (FIFTEEN SPECIMENS)	10.2-25.4
12.7	19.1	12.7	1.5	6.3	3.8	0.25	1.7-6.9 (EIGHT SPECIMENS)	19.1

ALL DIMENSIONS IN mm.

Figure 2. - Chevron-notch short bar fracture toughness test specimen.

ORIGINAL PAGE IS
OF POOR QUALITY

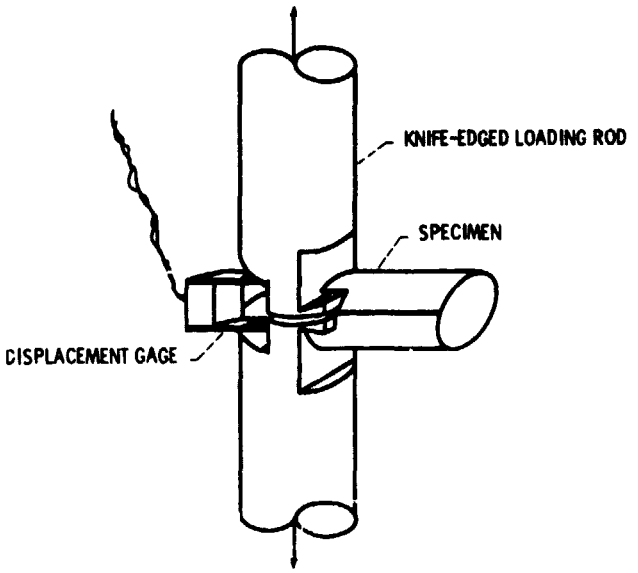

Figure 3. - Test setup.

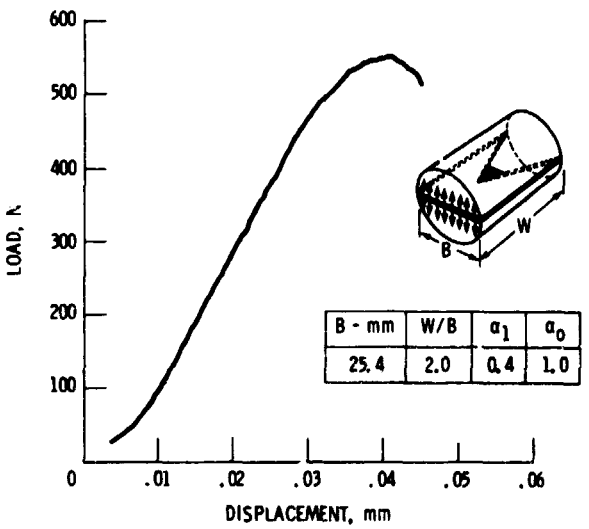

Figure 4. - Typical load versus displacement record for chevron-notch short rod specimen test of sintered aluminum oxide (Alsimag - 614).

ORIGINAL PAGE IS
OF POOR QUALITY

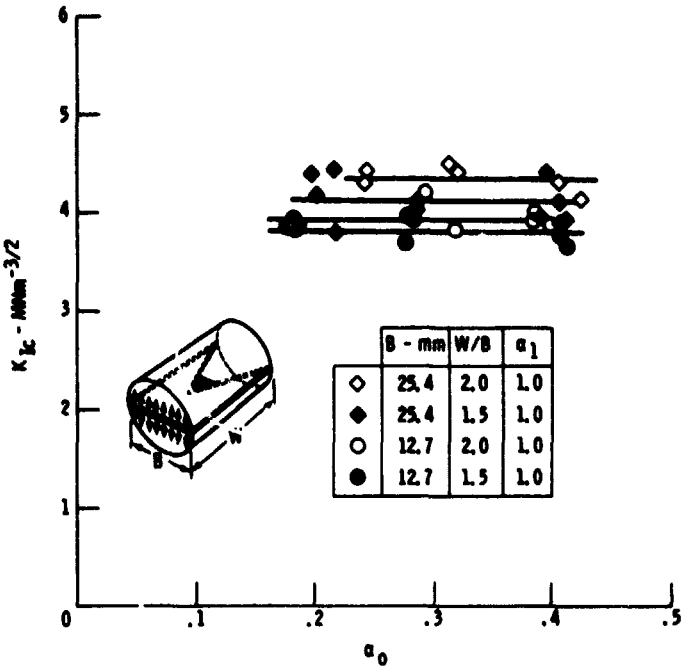

Figure 5. - Effect of a_0 on K_{Ic} of sintered aluminum oxide (Alsimag - 614) determined with chevron-notch short rod specimens.

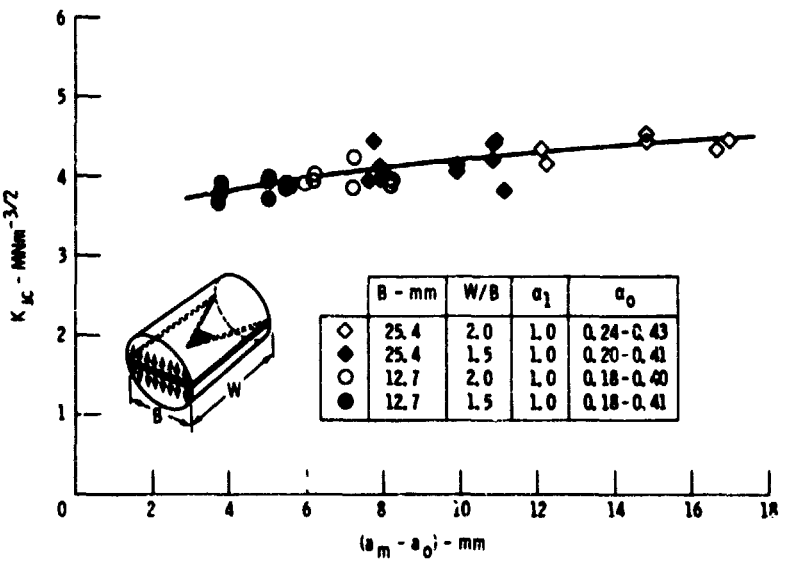

Figure 6. - Variation in K_{Ic} of sintered aluminum oxide (Alsimag-614) with amount of crack extension to maximum load for short rod chevron-notch specimens of a_1 = 1 in two diameters and W/B proportions, and variable chevron notch angle as obtained by varying a_0.

ORIGINAL PAGE IS
OF POOR QUALITY

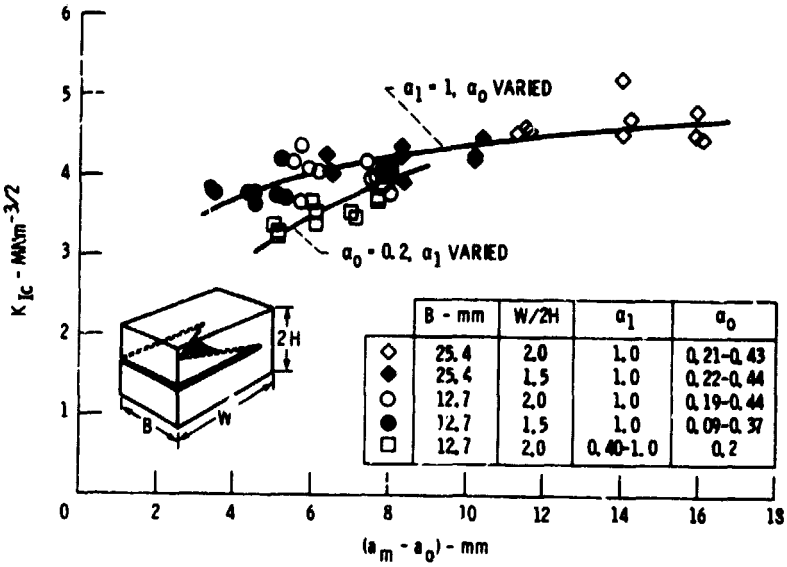

Figure 7. - Variation in K_{Ic} of sintered aluminum oxide (Alsimag-614) with amount of crack extension to maximum load for short bar chevron-notch specimen in two thicknesses and W/2H proportions, and variable chevron-notch angle attained by selectively varying either α_0 or α_1.

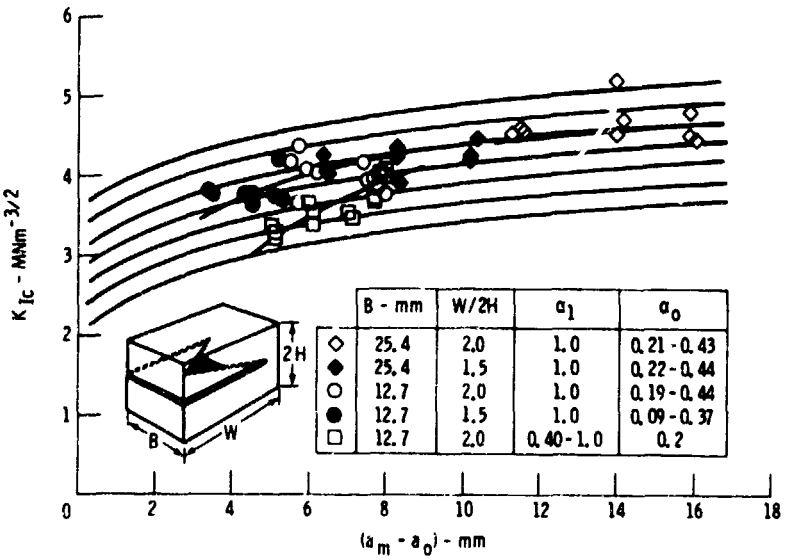

Figure 8. - Same as Figure 6 but with family of R-curves schematically overlain.

ORIGINAL PAGE IS
OF POOR QUALITY

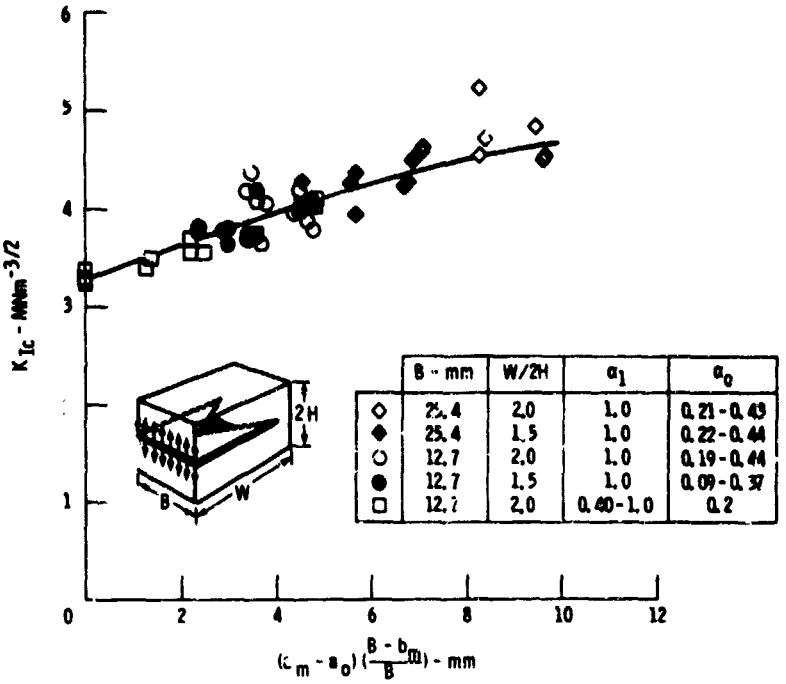

Figure 9. - Data of Figure 7 replotted with abscissa normalized to account for variable side grooving effect of the chevron notch.

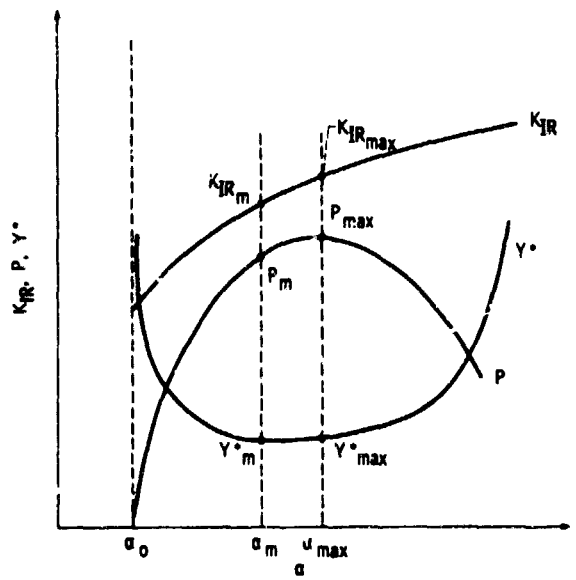

Figure 10. - Lack of coincidence between the load maximum and the stress intensity factor coefficient minimum values as functions of relative crack length for rising R-curve materials.